Journal of Power Sources 195 (2010) 6294–6300

Contents lists available at ScienceDirect

Journal of Power Sources

journal homepage: www.elsevier.com/locate/jpowsour

# Preparation of Ni–Fe bimetallic porous anode support for solid oxide fuel cells using $LaGaO_3$ based electrolyte film with high power density

Young-Wan Ju[a], Hiroyuki Eto[b], Toru Inagaki[c], Shintaro Ida[a], Tatsumi Ishihara[a,*]

[a] Department of Applied Chemistry, Faculty of Engineering, Kyushu University, Motooka 744, Nishi-Ku, Fukuoka 819-0395, Japan
[b] Mitsubishi Materials Corporation, Central Research Institute, 1002-14 Mukohyama, Naka-Shi, Ibaraki 311-0102, Japan
[c] The Kansai Electric Power Co., Inc., 11-20 Nakoji 3-Chome, Amagasaki, Hyogo 661-0974, Japan

ARTICLE INFO

*Article history:*
Received 4 March 2010
Received in revised form 16 April 2010
Accepted 21 April 2010
Available online 28 April 2010

*Keywords:*
Solid oxide fuel cell
Thin film
LSGM
Metal support
Pulsed laser deposition

ABSTRACT

Optimization of sintering temperature for $NiO–Fe_2O_3$ composite oxide substrate was studied in order to obtain a dense substrate with smooth surface. By in situ reduction, the substrate was changed to a porous Ni–Fe alloy metal. The volumetric shrinkage and porosity of the substrate were also studied systematically with the Ni–Fe substrate reduced at different temperatures. A Sr and Mg-doped $LaGaO_3$ (LSGM) thin film was prepared on dense substrate by the pulsed laser deposition (PLD) method. The LSGM film with stoichiometric composition was successfully prepared under optimal deposition parameters and a target composition. $Sm_{0.5}Sr_{0.5}CoO_3$ (SSC55) cathode was prepared by the slurry coating method on the deposited film. Prepared SOFC single cell shows high power density and the maximum power density (MPD) achieved was 1.79, 0.82 and 0.29 W $cm^{-2}$ at 973, 873 and 773 K, respectively. After thermal cycle from 973 to 298 K, the cell shows almost theoretical open circuit potential (1.1 V) and the power density of 1.62 W $cm^{-2}$, which is almost the same as that at first cycles. Therefore, the Ni–Fe porous metal support made by the selective reduction is highly promising as a metal anode substrate for SOFC using $LaGaO_3$ thin film.



## 1. Introduction

Among various types of fuel cells, solid oxide fuel cells (SOFCs) have been attracting much interest as a reliable power generator for the next generation due to their excellent fuel flexibility, long life, and highest energy efficiency [1–4]. Conventional SOFCs mainly consist of ceramic materials such as yttria-stabilized zirconia (YSZ) electrolyte, Mn-based perovskite cathode, and Ni–YSZ anode. Among the ceramic material, YSZ are used as electrolyte and ion pathway in anode due to its high oxygen ion conductivity at temperature higher than 1073 K. Therefore, the SOFCs using YSZ electrolytes have operated at higher temperature and have been considered as stationary generators such as power plants and combined heat-power generation (CHP) systems. Recently, operation at intermediate temperature is required in order to improve the reliability and service life. However the operation at low temperatures accompanies low power density due to the high internal resistance of YSZ electrolytes at low temperature. Therefore, various materials such as strontium and magnesium doped $LaGaO_3$ (LSGM), samarium doped ceria (SDC), and samarium doped $BaCeO_3$ have been considered as an electrolyte instead of YSZ. Among them, LSGM electrolytes have been extensively studied due to their higher oxide ion conductivity and also higher ionic transference number over a wide range of oxygen partial pressure [5–9].

In order to achieve excellent cell performance, it is important that the electrode should exhibit high activity to electrode reaction, thermal expansion property compatible with an electrolyte, and the sufficient porosity to achieve a sufficient three-phase boundary (TPB). Therefore, in current SOFC system, cermets consisting of Ni and ceramic oxide such as SDC, LSGM and YSZ have been used as an anode. In our previous works, we confirmed a small amount of Fe additive in the Ni substrate improved the catalytic activity and compatibility of thermal expansion with LSGM electrolyte [9]. However, the fracture property of ceramic material limits wider application of SOFC as ever. Therefore, metallic anode substrates have been suggested as alternative candidates to solve the problem of fragile property of cermets. However, the use of metal substrate accompanies low power generation property due to the decrease of TPB. In order to improve the power generation property, well-developed micro-pore and thin electrolyte is necessary for the expansion of TPB and the decrease of internal resistance. Till now, various methods such as spin coating [10], colloidal deposition [11], plasma spraying [12], electrostatic assisted vapor deposition [13], pulsed laser deposition (PLD) [8,9], and metal organic chemical vapor deposition [14] have been introduced to fabricate thin electrolyte. Among them, the PLD method is attracting much interest

* Corresponding author. Tel.: +81 92 802 2868; fax: +81 92 802 2871.
*E-mail addresses:* ju_w@cstf.kyushu-u.ac.jp (Y.-W. Ju), ishihara@cstf.kyushu-u.ac.jp (T. Ishihara).

0378-7753/$ – see front matter © 2010 Elsevier B.V. All rights reserved.
doi:10.1016/j.jpowsour.2010.04.068

due to its simple technique, easy control of film composition, uniformity in film thickness, and composition. In the previous study, we prepared a LSGM electrolyte film by the PLD method on cermets substrates. The SOFC cell prepared with this deposited film exhibits extremely high power density (>3 W $cm^{-2}$) and almost theoretical open circuit voltage (OCV) [8,9].

Therefore, in this study, we investigated the optimal preparation conditions of Ni–Fe bimetallic porous anode substrate for the metal support SOFCs. Thin $La_{0.9}Sr_{0.1}Ga_{0.8}Mg_{0.2}O_{3-\delta}$ (denoted as LSGM9182) electrolyte films have been deposited on the dense composite oxide substrate under optimized conditions for the PLD method. After deposition, the dense anode substrate was reduced to obtain the porous metal substrate in $H_2$ flow at different temperatures. In addition, the SOFC single cell performance was also investigated with $Sm_{0.5}Sr_{0.5}CoO_{3-\delta}$ (SSC55) cathode at intermediate temperature.

## 2. Experiment

10 wt% $Fe_2O_3$ coated NiO powder was prepared by a traditional impregnation method. $Fe(NO_3)_3{\cdot}9H_2O$ was dissolved in de-ionized water, and then NiO powder was added into the solution proportionately. After the evaporation of water, the obtained powder was calcined in a ventilated furnace at 673 K for 2 h to decompose nitrate acid and then fired at 1473 K for 6 h. To obtain a fine and uniform particle mixture, the mixed powder was ground for 1 h in ethanol using the ball-milling process with zirconia balls. After drying the slurry, the resulting powder was pressed into disks (20 mm in diameter) at 20 MPa. After iso-statically pressing at 48 MPa, the obtained disks were sintered at various temperatures (1623–1823 K) for 5 h. In order to achieve a uniform and nano-sized pore in the metal substrate, the successive reduction of NiO–$Fe_2O_3$ composite was adopted. The substrates were reduced at various temperatures (873–1073 K). After reduction, the porosity and volume shrinkage were measured by the Archimedes method and volumetric change, respectively.

LSGM9182 and SDC20 bi-layer films were deposited on the dense NiO–$Fe_2O_3$ substrate by the laser ablation method using the commercial equipment (PLD-7, PASCAL). Before deposition, the chamber was evacuated to a pressure lower than $1.3 \times 10^{-7}$ Pa and then adjusted to a designated oxygen pressure of 0.667 Pa, by introducing commercial oxygen without purification. The laser power and frequency were controlled at 180 mJ $pulse^{-1}$ and 10 Hz, respectively. The substrate was heated to 1073 K before deposition. Heating and cooling rate was 200 K $h^{-1}$. $Sm_{0.2}Ce_{0.8}O_2$ (denoted as SDC20, Daiichi Kigenso Kagaku Kogyo Co. Ltd., Japan) was deposited between LSGM9182 and the NiO–$Fe_2O_3$ substrate to prevent the reaction between LSGM9182 and NiO. After deposition, the films were post-annealed in air at 1073 K for 2 h to ensure a superior contact and the development of the crystal structure of LSGM. Composition of the resulting LSGM9182 and SDC20 films was confirmed by EDX. The XRD analysis revealed that the perovskite phase of LSGM9182 was formed in the thin film after deposition. $Sm_{0.5}Sr_{0.5}CoO_{3-\delta}$ (SSC55), the cathode material, was synthesized by a modified citric acid method. The cathode was prepared by a slurry coating and then fired at 1073 K for 30 min. In the mean time, Pt wire was connected on the LSGM9182 film near the cathode for a reference electrode.

The power generating property of a single cell was measured by the 4-probes method. Humidified $H_2$ (2.8 vol.% $H_2O$) and commercial oxygen were fed to the cell as fuel and oxidant, respectively. The gas flow rate was 100 ml $min^{-1}$. A constant current was applied by using a galvanostat (Hokutò Denko, HA-301) and the potential was measured with a digital multimeter (Advantest 6145). Electrode over-potential was estimated by the current interruption method. A current pulse was generated with a current pulse generator (Hokuto HC111) and the residual potential response was analyzed with a memory hicoder (Hioki 8835).

## 3. Results and discussion

### 3.1. Preparation of Ni–Fe metal anode substrate

Dense surface of NiO–$Fe_2O_3$ substrate is necessary to fabricate uniform and dense electrolyte films with few or less μm thickness. Therefore, optimal sintering temperature was investigated to fabricate dense NiO–$Fe_2O_3$ substrate. Fig. 1 shows SEM images of the surface of NiO–$Fe_2O_3$ disk prepared at different sintering temperatures. NiO–$Fe_2O_3$ substrates, which were sintered at temperatures lower than 1673 K, definitely show the gain boundary and the holes. The porous surfaces changed to dense surface by elevating the temperature. However, the substrates, which were obtained by sintering at temperatures higher than 1773 K, have rough surface because of the increase in a grain size.

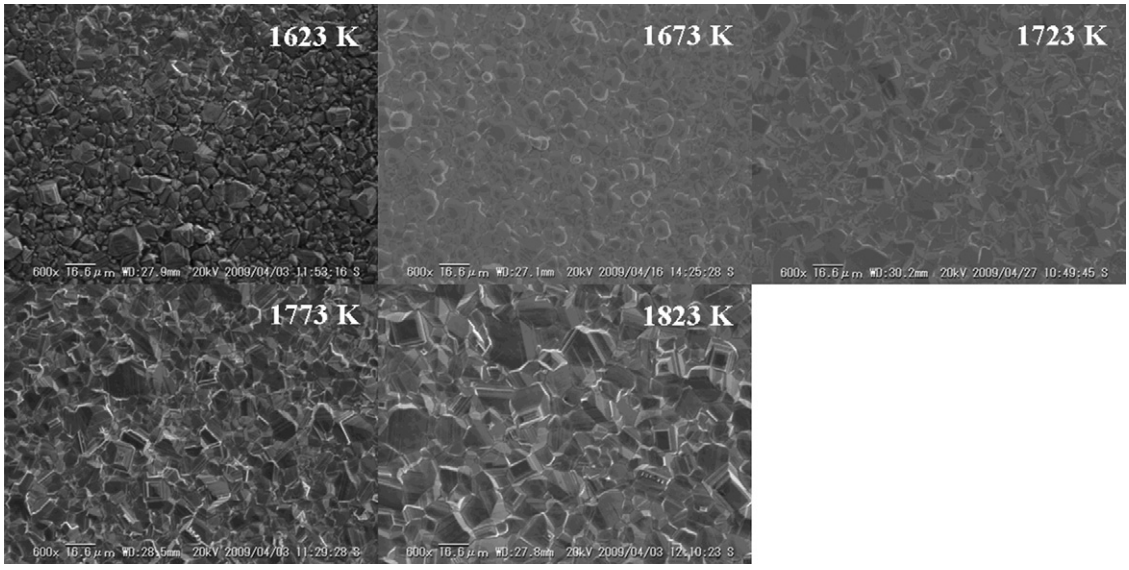


**Fig. 1.** Surface morphology of the NiO–$Fe_2O_3$ substrate sintered at different temperatures.

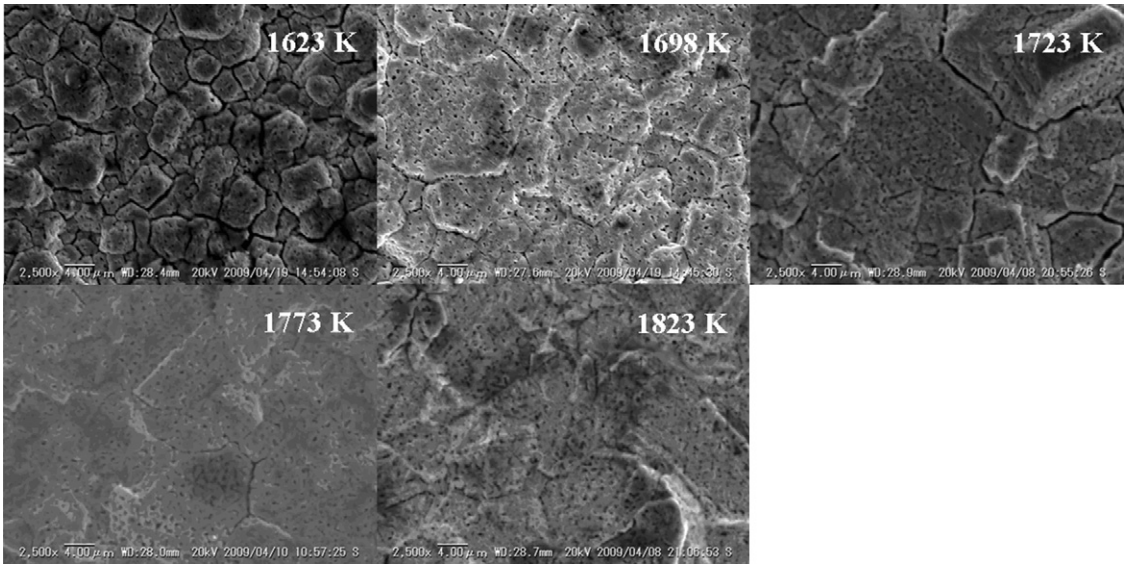


**Fig. 2.** SEM images of reduced Ni–Fe substrate prepared at different sintering temperatures.

As mentioned above, the porosity and shrinkage of substrate is important to obtain a metal support SOFC without gas-leakage. Therefore, to confirm the effect of sintering temperature on the porosity and shrinkage of metal substrate, the prepared substrates were reduced at 973 K in $H_2$ for 1 h ($H_2$ flow rate; 100 ml $min^{-1}$). Fig. 2 shows the SEM images of reduced Ni–Fe substrates at various temperatures. It is seen that small and uniform pores are randomly distributed on each grain. The Ni–Fe substrate sintered at low temperatures shows more definite grain boundary than those sintered at high temperatures. The growth of grain boundary is related to the shrinkage of grain. In the case of low temperature sintering, reduction and sintering of NiO–$Fe_2O_3$ particles were occurs simultaneously during the reduction. On the other hand, high temperature sintering leads to the dense substrate and after reduction, porosity becomes larger. Therefore, the shrinkage of substrates decreased as sintering temperature increases.

Table 1 summarizes the porosity measured by the Archimedes method and the shrinkage estimated by comparing the size of the disk before and after reduction. Effects of sintering temperature on porosity and shrinkage are also shown in Fig. 3. Evidently, substrates sintered at a higher temperature have larger porosity. The substrate prepared at 1773 and 1823 K had largest porosity but some cracks and the bending were observed. The leakage of gas takes place through these cracks and bending part under SOFC cell operation condition. On the other hand, porosity of the substrates was ca. 30% when sintering and reduction were performed at temperature lower than 1723 and 973 K, respectively. The porosity of 30% is slightly small for the porous substrate of SOFC; however, considering the $H_2$ permeation rate, it could be used as the porous substrates. The volumetric shrinkage during the reduction should be smaller as much as possible in order to prevent the formation of cracks and delaminating in the thin electrolyte film. The shrinkage was decreased by elevating the sintering temperature because the substrate prepared at a higher temperature formed a dense structure during the sintering process. Therefore, the optimum sintering temperature for the NiO–$Fe_2O_3$ substrate is 1723 K and reduction is 973 K.

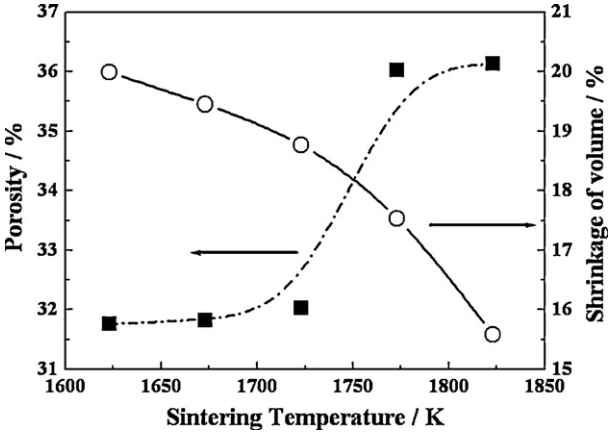


**Fig. 3.** Porosity and volumetric shrinkage of the anode substrate as the function of sintering temperature.

The reduction process changed the morphology and also structure of substrate. Fig. 4 shows X-ray diffraction (XRD) patterns of substrate before and after reduction. Before reduction, the substrate was consisted with NiO and $NiFe_2O_4$ phase. However, after

**Table 1**
Change of NiO–$Fe_2O_3$ substrate's volume and density by reduction.

| Sample (shrinkage, vol.%) | | Weight (g) | Volume ($cm^3$) | Density (g $cm^{-3}$) | Apparent density (g $cm^{-3}$) | Relate density | Porosity (%) |
|---|---|---|---|---|---|---|---|
| NiFe1623 | Before reduction | 1.99 | 0.35 | 5.88 | 6.11 | 96.30 | 3.70 |
| (19.99) | After reduction | 1.57 | 0.28 | 5.78 | 8.47 | 68.24 | 31.76 |
| NiFe1673 | Before reduction | 1.93 | 0.30 | 5.88 | 6.02 | 97.62 | 2.38 |
| (19.45) | After reduction | 1.52 | 0.24 | 5.77 | 8.46 | 68.17 | 31.83 |
| NiFe1723 | Before reduction | 2.02 | 0.35 | 5.88 | 5.98 | 98.33 | 1.67 |
| (18.77) | After reduction | 1.59 | 0.29 | 5.75 | 8.46 | 67.97 | 32.03 |
| NiFe1773 | Before reduction | 1.95 | 0.36 | 5.76 | 5.83 | 98.86 | 1.14 |
| (17.62) | After reduction | 1.53 | 0.29 | 5.69 | 8.90 | 63.97 | 36.03 |
| NiFe1823 | Before reduction | 2.03 | 0.37 | 5.73 | 5.78 | 99.12 | 0.88 |
| (15.58) | After reduction | 1.59 | 0.31 | 5.49 | 8.59 | 63.87 | 36.13 |

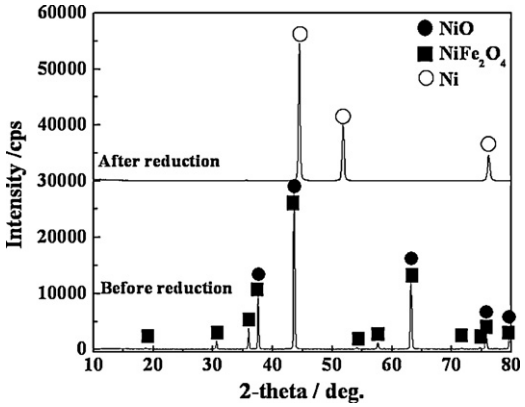


**Fig. 4.** XRD patterns of the Ni–Fe bimetallic anode before and after reduction.

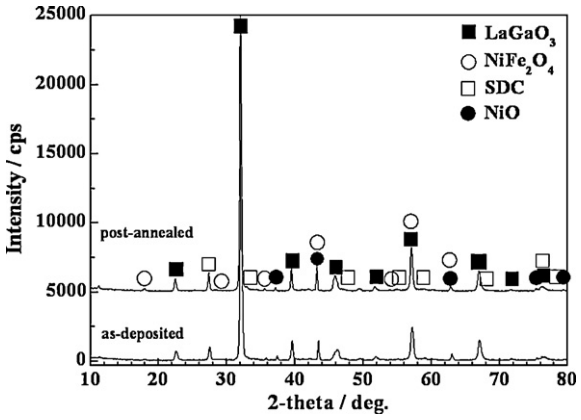


**Fig. 5.** XRD patterns of as-deposited and post-annealed $LaGaO_3$ film.

reduction, only shifted Ni diffraction peaks were observed. This result suggests that all composite oxides were reduced completely to metal and added Fe seems to form alloy with Ni. It is also noted that diffraction angle was shifted to lower angle by addition of Fe comparing with that of pure Ni. In according with the phase diagram [15], composition of Ni:Fe = 9:1 forms the alloy with FCC structure. Consisting with the phase diagram, Ni–Fe alloy is formed after reduction.

### 3.2. Preparation of LSGM/SDC bi-layer film by pulse laser deposition (PLD) method

Since LSGM consists of four elements, the control of the film composition is rather difficult for making film. Therefore, adjustment of film composition is highly important for the preparation of LSGM9182 film for electrolyte. It is well-known that the PLD method has an advantage of a small deviation in the composition from that of the target. However, as shown in Table 2, deviation of film composition from target one is observed. In particular, concentration of La and that of Mg tend to be high and low respectively. Therefore, the deposition parameters and the composition of the target were requested to be optimized to get a dense electrolyte film with stoichiometric composition. Table 2 shows the composition of the bulk LSGM9182 and the deposited LSGM9182 film analyzed with SEM–EDAX. The composition of the deposited film is almost the same as that of the bulk LSGM9182.

Fig. 5 shows the XRD patterns of the obtained $LaGaO_3$ film before and after annealing. It is seen that the perovskite phase of LSGM9182 and fluorite phase of SDC20 were successfully formed in the as-deposited film. Therefore, the perovskite structure of $LaGaO_3$ was already formed during deposition. Considering the intensity of each diffraction peak with those in JCPDS card (PDF: 40-1183), the relative density of the (1 1 2) plane, which is the strongest peak, is much higher than that of the other X-ray diffraction peaks. Therefore, it is considered that the obtained $LaGaO_3$ based film is oriented along the (1 1 2) plane and the oriented growth seems to occur during deposition by PLD. After the post-annealing treatment at 1073 K, there is no change in the diffraction patterns of $LaGaO_3$ oxide; however, the relative intensity of $CeO_2$ slightly decreased. Because of weak intensity and broaden peak of SDC film due to the thin thickness of the film, the lattice parameter of SDC cannot be discussed in details. However, decrement of X-ray diffraction peak from SDC can be explained by reaction or decreased crystallinity. Post-anneal treatment is generally effective for improving the crystallinity of the film and so some reaction between the SDC20 film and the substrate or LSGM9182 film may occur. However, except for the decrease in diffraction peak intensity from SDC20, there is no significant change observed in XRD patterns after the post-anneal treatment and no diffraction peaks from the secondary phase are observed. Therefore, no significant reaction occurred on the LSGM9182 and/or SDC20 film. In addition, the reaction between LSGM9182 and Ni was effectively prevented.

Fig. 6 shows the LSGM9182–SDC20 bi-layer film on the $NiO–Fe_2O_3$ anode substrate. Evidently, the surface of the deposited LSGM9182 film has a dense and gas-tight morphology without any cracks and pin-holes as shown in Fig. 6(a). In spite of rough surface, the uniform thickness of the film was obtained without any columnar structure. This suggests that the $NiO–Fe_2O_3$ is quite suitable substrate materials for obtaining dense LSGM9182 film by PLD method. It is also seen that the thickness of the deposited LSGM9182 film is around 6 μm and that of SDC20 is not clearly observed, but considering the deposition period, the thickness of SDC20 layer is estimated to be 500 nm.

### 3.3. Effect of reduction temperature on the power generation property

In order to confirm the optimal reduction temperature, dense $NiO–Fe_2O_3$ substrates were reduced at 873, 973, and 1073 K in $H_2$ for 1 h, respectively. Fig. 7 shows the surface morphologies of reduced $NiO–Fe_2O_3$ disks at various temperatures. It is seen that each grain consists of small and uniform pores. In the case of reduction at 873 K, there are large pore observed, which might be assigned to the formation of pin-holes. On the other hand, when the reduction temperature was higher than 973 K, the substrates with uniform and random pore were obtained. As mentioned above, large porosity and small shrinkage is necessary in order to obtained LSGM9182 film without crack. The reduced Ni–Fe substrate at 873 K

**Table 2**
Comparison of the composition of LSGM film and bulk LSGM9182 analyzed by EDAX.

| | La | | Sr | | Ga | | Mg | | Total |
|---|---|---|---|---|---|---|---|---|---|
| | at.% | Ratio | at.% | Ratio | at.% | Ratio | at.% | Ratio | |
| BulK LSGM9182 | 51.04 | | 2.46 | | 24.12 | | 22.38 | | 100.00 |
| LSGM film | 51.09 | 1.00 | 2.43 | 0.99 | 24.11 | 1.00 | 22.37 | 1.00 | 100.00 |

LSGM target, $La_{0.7282}Sr_{0.1}Ga_{0.6380}Mg_{0.4255}O_{3-\delta}$.

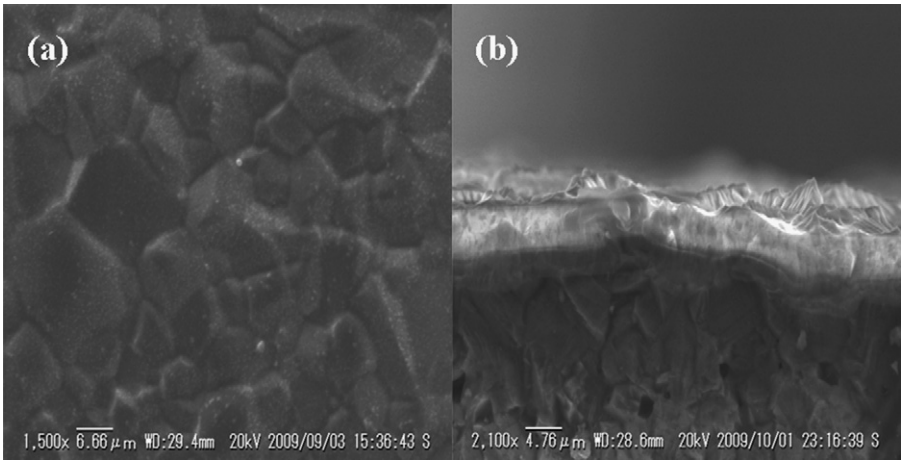


**Fig. 6.** SEM images of the deposited $LaGaO_3$ film; (a) surface morphology and (b) cross-section.

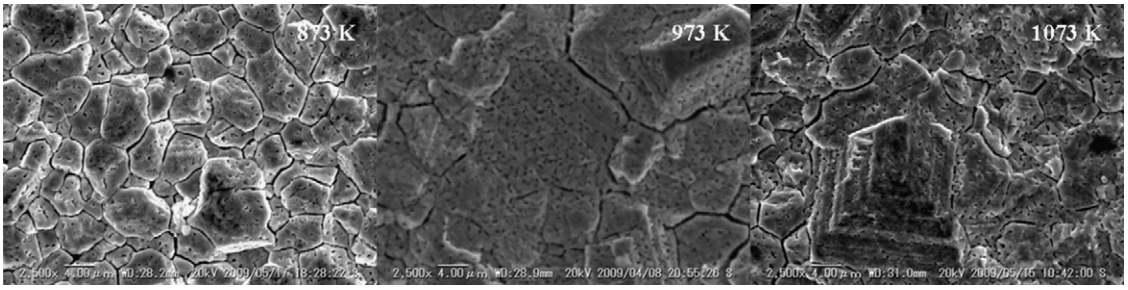


**Fig. 7.** SEM images of the Ni–Fe substrate reduced at different sintering temperatures.

has largest porosity and smallest volumetric shrinkage of 32.8% and 18.3%, respectively. However, this large porosity may occur by well-developed grain boundary as shown in Fig. 7. The porosity of substrate decreased with an increase in the reduction temperature. However, the porosity of all samples is larger than 30% and reasonably acceptable for the anode substrate of SOFC. On the other hand, the shrinkage of the substrate increased with an increase in the reduction temperature. Especially, the reduced substrate at 1073 K exhibits the largest shrinkage as large as 22.5% among examined temperature range. The shrinkage is occurred by the reduction of $NiO–Fe_2O_3$ composite oxide to metal phase. In according to the phase diagram [15], the Ni–Fe composite oxide (9:1 by the weight ratio) consists of two phase mixture of $(Ni_{0.95}Fe_{0.05})O$ and $(Fe_{0.7}Ni_{0.3})_3O_4$. The composite oxide is reduced to metal in the hydrogen atmosphere. During the reduction, the Ni rich phase, which is $(Ni_{0.95}Fe_{0.05})O$, is readily reduced comparing with the Fe rich one, which is $(Fe_{0.7}Ni_{0.3})_3O_4$. Therefore the reductions of two phase mixtures lead to the formation of micro-pores due to slow reduction of $(Fe_{0.7}Ni_{0.3})_3O_4$ and also this suppress the shrinkage. As a result, the reduction rate which relates with the reduction temperature is an important parameter for obtaining the thin film SOFC supported on the porous metal. It is considered that the larger shrinkage is brought about by the faster reduction rate, since $(Fe_{0.7}Ni_{0.3})_3O_4$ phase is simultaneously reduced with the $(Ni_{0.95}Fe_{0.05})O$ phase at high temperature. For more detail investigation into the effect of reduction temperature, three cells have been prepared and measured the power generation property after the reduction at different temperatures.

In order to measure the power generation property, the prepared cells were set between vertical alumina tubes with 17 mm diameter. For gas sealing, the molten Pyrex glass ring was used. After sealing at 1073 K, 2 h, gas-leakage was checked at 973 K by feeding $O_2$ and it is confirmed that all samples showed no gas-leakages. Fig. 8 shows the power generation properties of the SOFC single cell reduced at the different temperatures. The reduced cell at 973 K shows almost theoretical open circuit voltage (OCV) and high power density. On the other hand, the reduced cells at 873 and 1072 K show low OCV and the power density. These low values may originate from the fuel leakages, which is occurred by the crack or delaminating of electrolyte.

The formation of crack and delamination was confirmed with the SEM observation as shown in Fig. 9. After the measurement, the reduced cell at 973 K has dense surface. On the other hand, the cell reduced at 1073 K shows the delaminated electrolyte film. The crack and delaminating of deposited film was explained by the large shrinkage of the Ni–Fe substrate during the reduction process. As mentioned above, the shrinkage of reduced cell at 873 K was smallest than that at other temperature. However, the cell shows

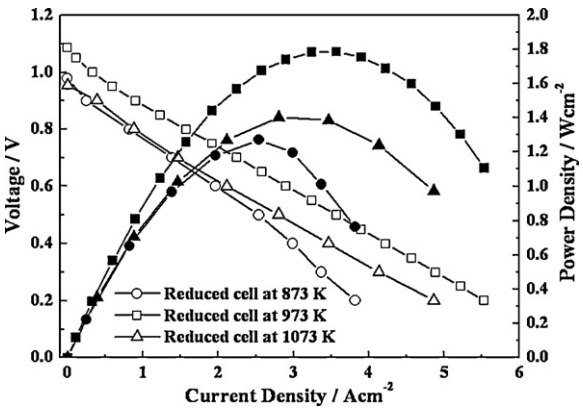


**Fig. 8.** Power generation property depends on reduction temperature at 973 K.

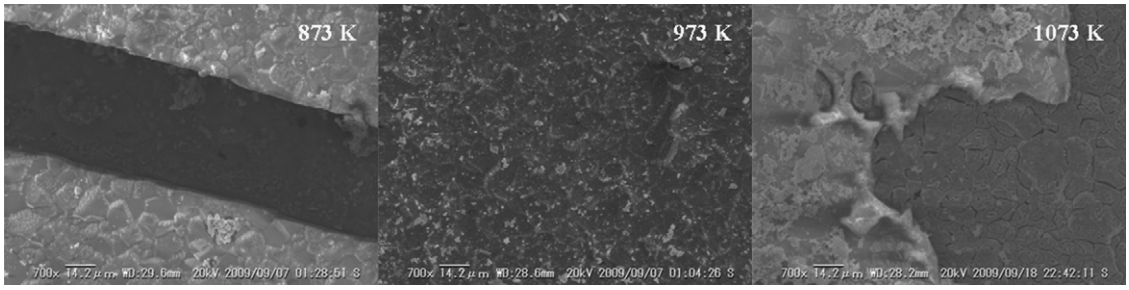


**Fig. 9.** The surface morphology of deposited film after the cell operation at 973 K.

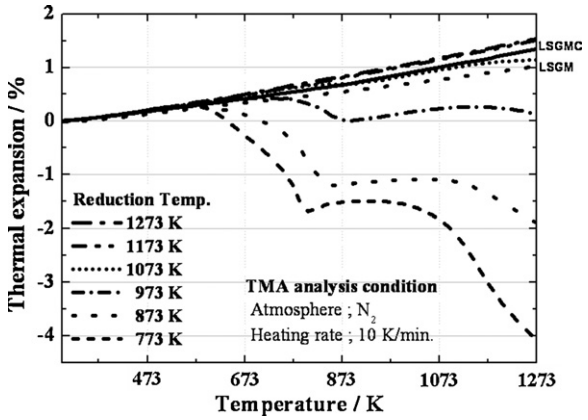


**Fig. 10.** Thermal expansion of the Ni–Fe substrate as a function of reduction temperature.

the crack of deposited film. This result is explained by the thermal expansion property of reduced Ni–Fe substrate. Fig. 10 shows the thermal expansion properties of reduced substrate at different temperatures. Ni–Fe substrate, which is reduced at temperature higher than 973 K, shows similar thermal expansion property with that of LSGM9182. However the substrates obtained by reduction at temperature lower than 973 K show the large shrinkage because of sintering. In case of metal substrate, the thermal expansion coefficient is generally much larger than that of ceramics. However, as shown in Fig. 10, mismatch in the thermal expansion coefficient is not large and this suggests that the porous metal substrate of Ni–Fe can be used as the substrate of LSGM9182 film.

Fig. 11 shows the power generating property of the cell reduced at 973 K. It is seen that the maximum power density was achieved to a value of 1.79, 0.82 and 0.29 W $cm^{-2}$ at 973, 873 and 773 K, respectively. The power density decreased by decreasing temperature. However, OCV was almost theoretical value at each temperature. It shows that thin LSGM9182 film electrolyte keep dense morphology in the change of temperature. In addition, there is no concentra-

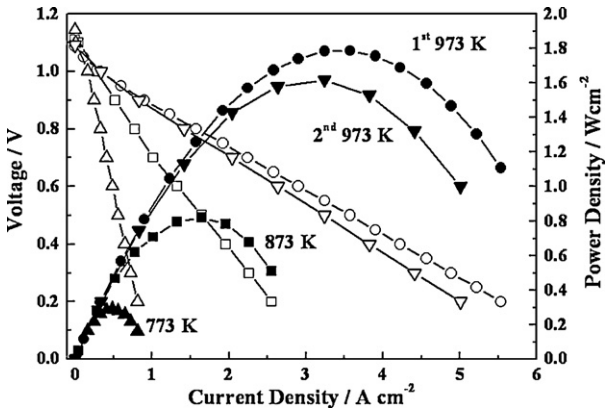


**Fig. 11.** Power generating property of the cell using LSGM/SDC bi-layer film as electrolyte.

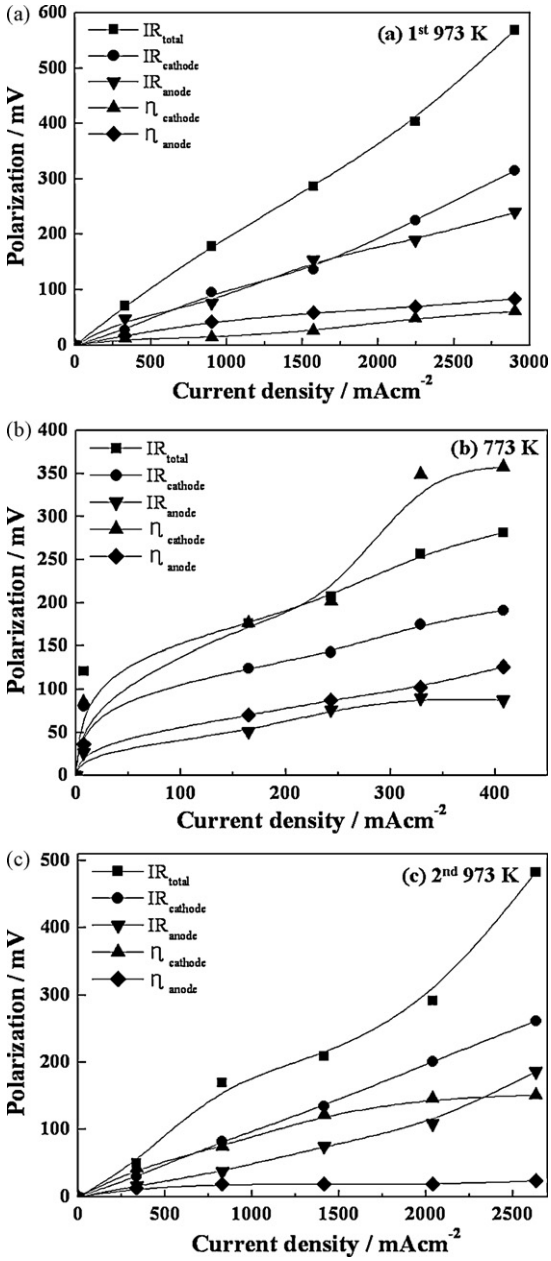


**Fig. 12.** Internal resistance of the Ni–Fe metal supported LSGM cell at (a) 973 K, (b) 773 K and (c) 973 K after thermal treatment.

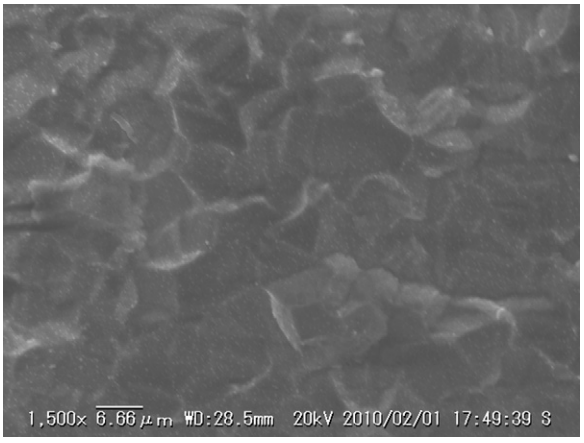


**Fig. 13.** Cross-section image of the Ni–Fe metal supported LSGM cell after the cell operation.

tion over-potential observed on the *I–V* curves. Therefore, it can be said that the porosity of the metal substrate is high enough for the SOFC with a porous anode substrate. Moreover, the effects of thermal cycling treatment on the cell performance were further studied and the results are shown in Fig. 11. After thermal treatment, the cell shows the high OCV and large power density of 1.62 W $cm^{-2}$. The results showed high mechanical toughness, which is one of the great advantages of metal support SOFC. However, the decrease in power density about 10% was observed after the thermal cycling treatment. In order to identify the decreased power density after thermal cycling treatment, internal resistance analysis and SEM observation was performed.

Fig. 12 shows the internal resistance of the Ni–Fe metal supported LSGM9182 cell. Because the resistance of the film is small, there is a possibility that reference electrode at cathode is short circuited to anode substrate. However, in this study, we tentatively tried to separate the anodic and cathodic resistance by a current interruption method. Although the thickness of the LSGM9182 electrolyte film is as thin as 6 μm, the internal resistance of the cell is still dominated by the IR loss. However, at 773 K, cathodic over-potential is larger than IR loss. Moreover, the cathodic over-potential after 2nd thermal cycle treatment is larger than that at 1st cycle. Increase in the cathodic over-potential may be occurred by sintering or delamination of cathode. Since the cathode was calcined at 1073 K, delamination seems to be more reasonable because of highly smooth surface of the film and the insufficient mechanical strength of cathode by low temperature calcinations (1073 K). Therefore, by decreasing the over-potential in the cathode part, the maximum power density of the cell could be further improved.

Fig. 13 shows the SEM image of the surface morphology of cell after thermal cycling test. After the cell operation, the electrolyte was still quite dense without any cracks or pin-holes. Therefore, it can be said that LSGM9182 film on Ni–Fe porous metal substrate is highly strong against thermal cycling treatment and useful for a reliable SOFC, which is non-fragile. The poor thermal cycle durability might be explained by delamination of cathode and thermal cycling.

## 4. Conclusion

Effects of sintering and reduction temperature on porous metal substrate were investigated for metal support SOFC. The porosity was increased and the volumetric shrinkage was suppressed by increasing sintering temperature. However, sintering temperature higher than 1773 K formed cracks and bending of substrate. Therefore, a thin LSGM9182 film was prepared on the NiO–$Fe_2O_3$ substrate sintered at 1723 K. The film has a similar composition as that of bulk LSGM9182 and is highly dense without pin-holes or cracks. After the in situ reduction of NiO and $Fe_2O_3$ at 973 K, porous alloy substrates were successfully obtained. In addition, the SOFC single cell with the SSC55 cathode was operated at a relatively low temperature and exhibited a fairly large power density. After the thermal treatment, power density slightly decreased, however, the maximum power density is as high as 1.62 W $cm^{-2}$. DC polarization measurements revealed that the anode over-potential is not significant; however, the IR loss and over-potential at cathode side dominated the cell performance at low temperature (773 K). It is considered that the SOFC cell performance could be further elevated by improvement of cathode morphology. In addition, after the thermal cycle treatment, cathodic over-potential increased. The poor thermal cycle stability seems to be originated from the delamination of $SmCoO_3$ based oxide cathode because of the insufficient mechanical strength. However, LSGM9182 film on the porous Ni–Fe metal substrate is still dense and no crack forms after thermal cycling test. Therefore, cell performance as well as reliability of the cell against thermal cycle could be much improved by improving the mechanical property of cathode. Consequently, this study reveals that the selective reduction of NiO–$Fe_2O_3$ is highly useful for making metal support SOFC cell and that the resulting Ni–Fe porous support is highly compatible with LSGM9182 electrolyte film.

## References

[1] S.C. Singhal, Solid State Ionics 152–153 (2002) 405.
[2] N.Q. Minh, Solid State Ionics 174 (1–4) (2004) 271.
[3] O. Yamamoto, Electrochim. Acta 45 (15–16) (2000) 2423.
[4] W.Z. Zhu, S.C. Deevi, Mater. Sci. Eng. A 362 (1–2) (2003) 228.
[5] T. Ishihara, H. Matsuda, Y. Takita, J. Am. Chem. Soc. 116 (9) (1994) 3801.
[6] T. Ishihara, H. Minami, H. Matsuda, H. Nishiguchi, Y. Takita, Chem. Commun. 8 (1996) 929.
[7] T. Ishihara, M. Honda, T. Shibayama, H. Minami, H. Nishiguchi, Y. Takita, J. Electrochem. Soc. 145 (9) (1998) 3177.
[8] J.W. Yan, H. Matsumoto, M. Enoki, T. Ishihara, Electrochem. Solid-State Lett. 8 (8) (2005) A389.
[9] T. Ishihara, J.W. Yan, M. Shinagawa, H. Matsumoto, Electrochim. Acta 52 (4) (2006) 1645.
[10] C.C. Chen, M.M. Nasrallah, H.U. Anderson, Solid State Ionics 70–71 (1994) 101.
[11] S. de Souza, S.J. Visco, L.C. De Jonghe, Solid State Ionics 98 (1–2) (1997) 57.
[12] C. Lunot, Y. Denos, in: D.A. Dolenc (Ed.), Proceeding of the 1998 International Gas Research Conference, Gas Research Institute, Chicago, IL, 1998, p. 834.
[13] H. Nagamoto, H. Ikewaki (Eds.), Mat. Res. Soc. Symp. Proc., vol. 547, Materials Research Society, Warrendale, 1999, p. 333.
[14] W. Bai, K.L. Choy, R.A. Rudkin, B.C.H. Steele, Solid State Ionics 113–115 (1998) 259.
[15] Phase Diagram, American Ceramic Society, Fig. 5421.